Central Lancashire Online Knowledge (CLoK)

Title	Performance of green high-strength concrete incorporating palm oil fuel ash in harsh environments
Type	Article
URL	https://clok.uclan.ac.uk/51081/
DOI	##doi##
Date	2024
Citation	Zeyad, Abdullah M., Johari, Megat Azmi Megat, Aliakbar, Ali, Magbool, Hassan M., Majid, Taksiah A. and Aldahdooh, Majed A. A. (2024) Performance of green high-strength concrete incorporating palm oil fuel ash in harsh environments. Materials Science-Poland, 41 (4). pp. 24-40. ISSN 2083-134X
Creators	Zeyad, Abdullah M., Johari, Megat Azmi Megat, Aliakbar, Ali, Magbool, Hassan M., Majid, Taksiah A. and Aldahdooh, Majed A. A.

It is advisable to refer to the publisher's version if you intend to cite from the work. ##doi##

For information about Research at UCLan please go to http://www.uclan.ac.uk/research/

sciendo

Performance of green high-strength concrete incorporating palm oil fuel ash in harsh environments

Abdullah M. Zeyad[1,*], Megat Azmi Megat Johari[2], Ali Aliakbar[2], Hassan M. Magbool[1], Taksiah A. Majid[2], Majed A. A. Aldahdooh[3]

[1]Civil Engineering Department, College of Engineering, Jazan University, Jazan 45142, Saudi Arabia

[2]School of Civil Engineering, Universiti Sains Malaysia, Engineering Campus, 14300 Nibong Tebal, Penang, Malaysia

[3]International College of Engineering and Management Affiliated with University of Central Lancashire (UK), Muscat, Sultanate of Oman

The corrosion of steel reinforcement by chloride is commonly recognized as a key factor that contributes to the degradation of durability in reinforced concrete structures. Using supplementary cementitious materials, such as industrial and agricultural waste materials, usually enhances the impermeability of the concrete and its corrosion resistance, acid resistance, and sulfate resistance. This study's primary purpose is to examine the effects of replacing ordinary Portland cement (OPC) with ultrafine palm oil fuel ash (U-POFA) on the corrosion resistant performance of high-strength green concrete (HSGC). There were four HSGC mixes tested; the first mix contained 100% OPC, while the other mixes replaced OPC mass with 20%, 40%, and 60% of U-POFA. The performance of all HSGC mixes containing U-POFA on workability, compressive strength, porosity, water absorption, impressed voltage test, and mass loss was investigated at 7, 28, 60, and 90 days. Adding U-POFA to mixes enhances their workability, compressive strength (CS), water absorption, and porosity in comparison with mixes that contain 100% OPC. The findings clearly portrayed that the utilization of U-POFA as a partial alternative for OPC significantly enhances the corrosion-resistant performance of the HSGC. In general, it is strongly advised that a high proportion of U-POFA be incorporated, totaling 60% of the OPC content. This recommendation is the result of its significance as an environmentally friendly and cost-effective green pozzolanic material. Hence, it could contribute to the superior durability performance of concrete structures, particularly in aggressive environmental exposures.

Keywords: *corrosion resistance, high-strength green concrete, impressed voltage test, palm oil fuel ash, mass loss*

Graphical abstract
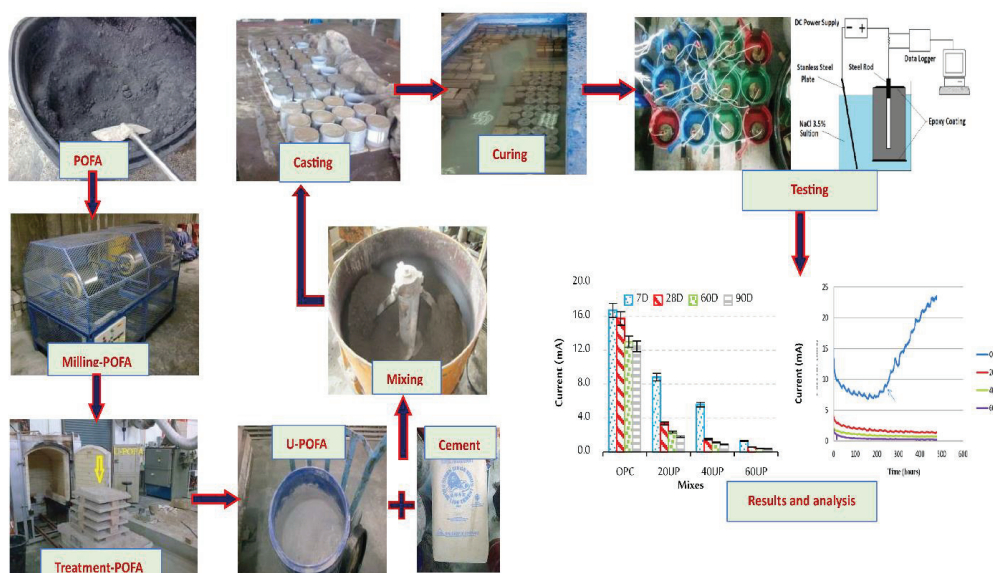
* E-mail: azmohsen@jazanu.edu.sa

Highlights

- The corrosion resistance performance of high-strength green concrete was investigated.
- Ultrafine palm oil fuel ash as a partial alternative of cement mass with 20%, 40%, and 60% was used.
- HSGC performance was evaluated in terms of workability, compressive strength, water absorption, porosity, impact stress testing, and mass loss.

1. Introduction

The yearly cost of repairing and rehabilitating reinforced concrete structures in the United States is assessed at a whopping $20 billion. It has been found that roughly 40% of this cost is associated with the corrosion of embedded rebar [1]. The corrosion of embedded steel rebars is a critical determinant affecting the durability and longevity of reinforced concrete. The steel rebars within concrete constructions are safeguarded against corrosion by the presence of an anti-rust coating, low permeability, low porosity, and high resistance to chemicals in alkaline concrete [2]. The exterior atmosphere and circumstances have a significant impact on the durability of reinforced concrete. The corrosion of steel reinforcement by chloride is commonly recognized as a primary factor contributing to the deterioration of durability in reinforced concrete [3]. The corrosion of embedded steel rebars in reinforced concrete can be classified into two distinct categories: direct corrosion, which occurs through metal oxidation or attack of acid, and indirect corrosion, which takes place through electrochemical reaction. The corrosion phenomenon found in steel rebars results in a decrease in their size and the formation of by-products that have a larger volume compared to the original size. Corrosion is a prevalent phenomenon that arises when steel rebars are subjected to the combined effects of water and oxygen. This chemical reaction results in the creation of iron oxide, resulting in an increase in volume. The volume expansion of steel during the corrosion

process is determined by the level of oxidation, with a maximum increase of 6.5 times [4]. The occurrence of this phenomenon induced tensile stresses inside the concrete matrix, resulting in the creation of cracks between the concrete and its reinforcement bars. The occurrence of rebar corrosion can be attributed to a range of conditions, encompassing temperature fluctuations, levels of humidity, salinity levels, and chemical reactions. The control and prevention of these conditions have significance because of the pivotal role that corrosion of steel bars plays in determining the durability and structural integrity of construction. Modifications made to the composition of the concrete mix design can have a substantial impact on the process of chloride ingress. The durability of concrete subjected to exterior chlorides is primarily influenced by the structure of the pores in the hardened cement paste [5]. The concrete mix design's key factors that significantly impact the diffusion coefficient of concrete are the ratio of the water to the cementitious material, the concrete's maturity during initial chloride exposure, and the inclusion of supplementary cementitious materials (SCMs) [1]. For several decades, many researchers have been employing industrial and agricultural waste materials such as silica fume (SF), palm oil fuel ash (POFA), and so forth, as SCMs to replace cement (OPC) in the production of concrete [6]. In addition to industrial and plant waste, eggshells are currently being used a SCMs [7]. These SCMs usually enhance the impermeability of the concrete and its corrosion resistance, resistance to acid, and resistance sulfate [8]. POFA is a promising byproduct-based pozzolan available in different parts of the globe. It is produced by burning empty fruit bunches, palm kernel shells, and palm fibers at $800°C–1000°C$ [9]. In Malaysia alone, for instance, the production of POFA rose from 3×10^6 tons in 2007 [10] to 4×10^6 tons in 2010 [11], and it is still on the increase today. Thailand also produces around 100,000 tons of POFA every year [12]. When pulverized into an ultrafine particle size (referred to as U-POFA), POFA has been seen to have a positive influence on the mechanical and fluid transport properties of concrete, leading towards improvements in its mechanical and

durability characteristics [13]. Incorporating ultra-fine materials with active pozzolanic properties such as U-POFA contributes to reducing permeability and improving the super-durability performance of concrete structures, especially in harsh environmental exposures [14]. Additionally, the use of POFA in concrete production has been found to facilitate the development of high-strength green concrete (HSGC) and ultra-high-strength concrete [14]. Jaturapitakkul et al. [15] reported that the use of POFA with higher fine particles improves the concrete's ability to withstand expansion caused by sulfate attack and increases its compressive strength (CS). Chandara et al. [16] mentioned that the larger particle size of POFA has a low rate of pozzolanic reactivity. Johari et al. [14] discovered that using U-POFA (2.06 μm) proved to be very effective as a strong pozzolanic ingredient in creating high-strength concrete (HSC) with exceptional durability. Raising the slump enhances fresh concrete properties and delays setting times, resulting in reduced chloride permeability and porosity of the HSC. Zeyad et al. [17] conducted an experimental study investigating the utilization of U-POFA in concrete with the objective of enhancing the CS. The researchers reported that the utilization of U-POFA has a significant function in enhancing the workability, impermeability, and strength characteristics of HSGC. The CS values obtained at 180 days were around 108, 114, and 112 MPa for the HSGC mixes containing 20%, 40%, and 60% of U-POFA, respectively. According to Thomas et al. [18], the utilization of POFA as a partial substitute for OPC resulted in a decrease in the permeability of concrete leading towards lower penetration of chloride ions, while at the same time increase the CS. Hamada et al. [19] carried out several investigations related to the utilization of POFA as a partial alternative for OPC in the production of environmentally friendly concrete. The researchers reached the conclusion that employing POFA with a fine particle size as a sustainable construction material offers several benefits to concrete specimens, particularly in terms of improving their strength and durability characteristics [20]. Alsubari et al. [21] conducted a study using the rapid chloride permeability test.

They used different amounts (30%, 50%, and 70%) of treated POFA instead of OPC in self-compacting concrete. The findings of the study demonstrated that the self-compacting concrete (SCC) containing treated POFA showed notable resistance to chloride ion penetration based on chloride permeability testing and superior strength retention at elevated temperatures. Furthermore, the SCC containing treated POFA surpassed the control SCC in terms of its performance. Furthermore, Alani et al. [22] noted that the incorporation of U-POFA and polyethylene terephthalate fiber resulted in the development of a high-performance concrete exhibiting exceptional resistance to the penetration of chloride ions after 7 days. At the age of 28 days, the resistance was reported to be significantly elevated. The durability of concrete is compromised when it is subjected to aggressive acidic conditions. Alsubari et al. [23] conducted an investigation of the chemical resistance of concrete incorporated with treated POFA by immersing concrete cubes (100 mm) in a solution of hydrochloric acid with a concentration of 3%. The experimental results indicated that the samples containing treated POFA exhibited high resistance to hydrochloric acid solutions compared to those composed of OPC. Bassuoni and Nehdi [24] demonstrated that the impact of a sulfuric acid attack can be more severe than a sulfate attack, mostly attributed to the dissolution impact caused by hydrogen ions and sulfate ions. In addition, Zeyad et al. [25] conducted an assessment of the transport characteristics of HSGC containing U-POFA. The study's results showed that the addition of U-POFA led to a significant decrease in chloride penetration and migration. This was due to the pozzolanic reaction of U-POFA, resulting in enhanced strength properties. Hassan et al. [26] achieved comparable findings in their investigation of the fluid transport characteristics of U-POFA-incorporated fiber-reinforced green concrete. To the best of the authors' knowledge, however, no study has investigated the corrosion resistance of HSGC when the U-POFA is added via the impressed voltage test and mass loss. Therefore, the aim of this study is to evaluate the effect of U-POFA on the corrosion resistance performance of HSGC. Also, the

physical and mechanical properties of HSGC containing U-POFA were investigated at 7, 28, 60, and 90 days.

2. Experimental study

2.1. Materials

The concretes in this study were produced using OPC river sand fine aggregate, granite coarse aggregate, U-POFA, and superplasticizer.

2.1.1. Cement

The cement) (OPC employed in this study was OPC Type 1, as specified by ASTM-C150 [27]. The OPC, a product of Cement Industries of Malaysia Berhad, with a specific gravity of 3.15.

2.1.2. Aggregates

The fine aggregates were natural river sand with a specific gravity of 2.75, water absorption of 0.61%, and a fineness modulus of 3.10, complying with the requirements of ASTM-C128 [28] and ASTM-C136 [29]. The coarse aggregate used was granite crushed with a maximum size of 12.5 mm, and the bulk density was 1550 kg/m^3, according to ASTM-C29 standard [29]. The specific gravity was 2.7, and water absorption was 0.49%, based on ASTM-C127 [30]. A sieve analysis was conducted on aggregates in order to generate the gradation curves according to ASTM-C33/C33M [31], as depicted in Figure 1.

2.1.3. Steel bars

This investigation involved the utilization of a typical steel bar (rod) of 10.0 mm in diameter for the purpose of conducting corrosion tests, simulating the conditions experienced by embedded steel within a HSC specimen. In this particular scenario, in order to achieve precise outcomes, it is imperative to pre-clean the steel rods. Consequently, the cleaning procedure was implemented in the following manner: Initially, the steel rods underwent a brushing process using an electrical brush equipped with a broad wired head. Subsequently, in order to eliminate any oil or other contaminants, the bars underwent a washing process with acetone, followed by a thorough drying using a pristine towel. Figure 2 depicts the steel bars utilized in this study, showcasing a visual contrast between their condition prior to the cleaning phase and their condition following the cleaning phase.

2.1.4. Chemical admixture

In this investigation, a chemical admixture known as GLENIUM ACE 393 superplasticizer, manufactured by BASF Chemical Company, was used. The primary objective of including this admixture was to decrease the water/cement ratio and enhance the workability of the HSGC. As per the manufacturer's specifications, the product is classified as a high-range water reducer and has been manufactured as Type F based on the criteria for an ASTM-C496 [32].

2.1.5. Palm oil fuel ash

This study utilized the procedure previously introduced by Johari et al. [13] for the production of the U-POFA. The original POFA (O-POFA) was obtained from a local palm oil mill in Penang, Malaysia. It was then dried in an electric oven at $100 \pm 5°$C for 24 hours to eliminate any moisture. The dried O-POFA was then passed through a 300-μm sieve to separate out the larger particles. Afterwards, the O-POFA underwent grinding, using a ball milling to create the ground POFA (G-POFA). The G-POFA was then heated in a furnace at 500°C for 90 min to reduce the unburnt carbon content and produce the treated POFA (T-POFA). Finally, the T-POFA was further ground in the same ball milling machine to obtain the U-POFA. The uniformity and consistency of the U-POFA produced were controlled by taking several measures, such as the amount of POFA put in the ball milling machine, the milling speed, the grinding time, the quantity of the POFA in the furnace, the heating time, and the heating temperature. The production process of the U-POFA is depicted in Figure 3.

2.2. Mixture proportions

In this study, the initial target strength for the concrete specimens across all groups was set to be a minimum of 80 MPa at 28 days with a 0.22 water-binder ratio (W/B ratio). Four concrete mixes were prepared with the proportions presented in Table 1.
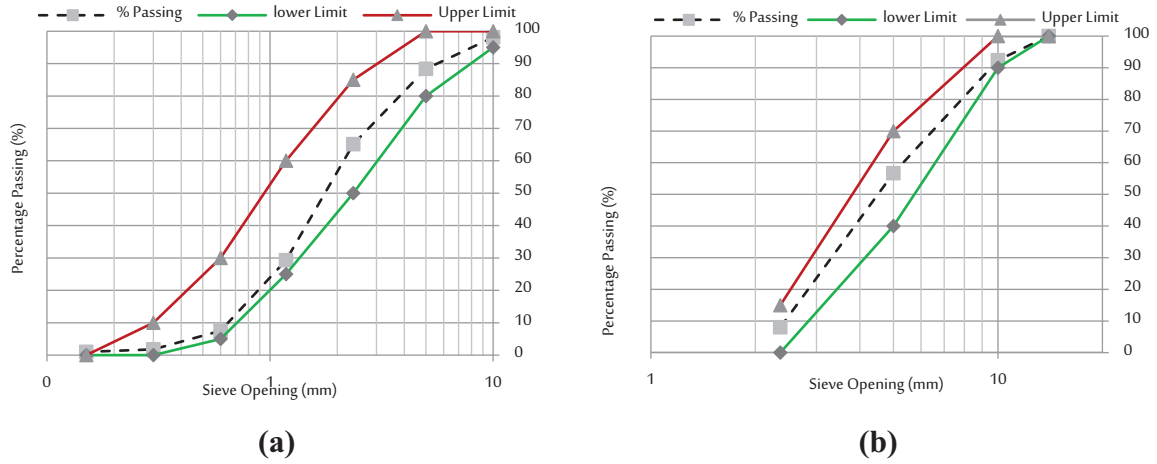
(a)   **(b)**

Fig. 1. Sieve analysis curves: (a) fine aggregate; (b) coarse aggregate

Fig. 2. The steel bar before and after the cleaning phase

Table 1. The concrete mix proportions in kg/m^3

Mix	Water	OPC	U-POFA	Aggregate		SP
				Coarse	Fine	
OPC	154	550	–	933	842	12.1
20UP	154	440	110	933	842	12.1
40UP	154	330	220	933	842	12.1
60UP	154	220	330	933	842	12.1

Abbreviations: OPC, Portland cement; 20UP, 20%
replacement with U-POFA; 40UP, 40% replacement
with U-POFA; 60UP, 60% replacement with U-POFA.

The first mix was the control with 100% OPC,
while the OPC was replaced with various ratios of
U-POFA in other mixes. Three replacement ratios
of U-POFA were used: 20% (20UP), 40% (40UP),
and 60% (60UP), as shown in Table 1. The mixing
procedure commenced by introducing the prede-
termined quantities of fine and coarse aggregates
into the pan-type mixer. Subsequently, the OPC or
binder was included in order to facilitate thorough
mixing. The duration of this step typically ranges
from three to four minutes, during which the aggre-
gates and binder are thoroughly mixed to achieve
a homogeneous dry mix. Subsequently, the water
and the superplasticizer (SP) were included in the
mixture, and the mixing procedure was sustained
for a duration of approximately four to six minutes.

2.3.   Specimen preparation

The concrete mixture was placed in the molds in
three layers, and then subjected to shaking using a
vibrating table to eliminate air bubbles and obtain a
homogeneous mixture. The molds were allowed to
sit for a period, after which they were then covered
with a moist, dense fabric and permitted to harden
for a duration of 24 hours. On the subsequent day,
the specimens were extracted from the molds and
subsequently immersed in a water tank for curing
purposes. The samples were then left to cure for
specified periods of 7, 28, 60, 67, and 90 days.

2.4.   Test methods

2.4.1.   Physical and chemical properties of U-POFA

Numerous analyses were conducted to inves-
tigate the alterations in physical properties and

O-POFA → Dry → **O-POFA in electrical oven**

O-POFA before sieving → Sieve → **O-POFA in electrical oven**

Ball milling machine → O-POFA milling → **G-POFA**

T-POFA before milling in final step → T-POFA milling → **The final product U-POFA**

Fig. 3. Production of U-POFA
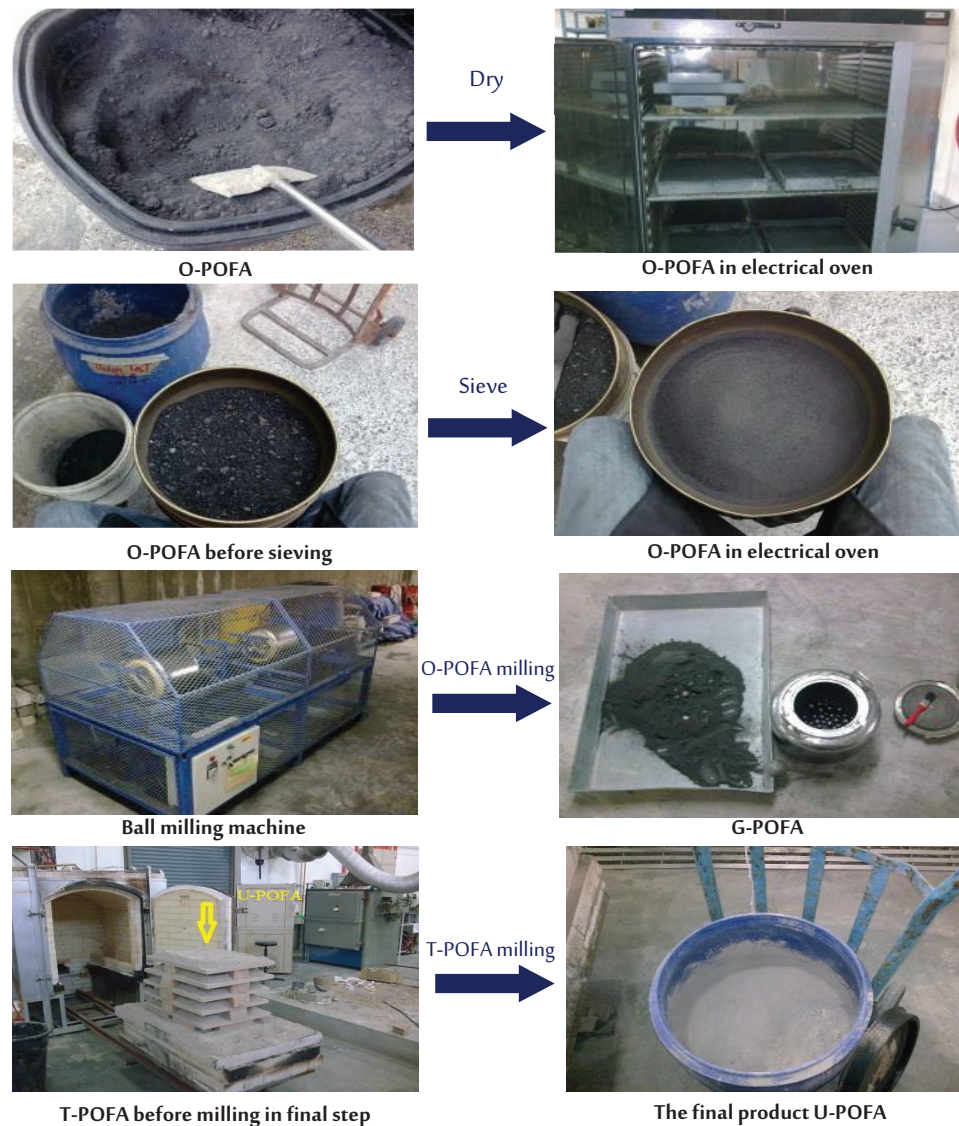
chemical compositions of POFA resulting from the treatment processes. The observation of changes in POFA properties was conducted using a scanning electron microscope (SEM). In addition, the chemical compositions were acquired using a nondestructive X-ray (XRF) method.

2.4.2. Compressive strength

The compressive test was performed on concrete cubes measuring 100 mm in size. The testing was applied at three different ages of 7, 28, and 90 days, in accordance with the specifications outlined in BS EN [33]. Results for each mix are calculated as average values derived from three cube results.

2.4.3. Water absorption and porosity

The water absorption and porosity tests were carried out in accordance with the ASTM-C373 [34] approach in this study. The samples were extracted with a diameter of 55 mm and a thickness of 40 ± 2 mm from concrete prisms measuring $100 \times 100 \times 500$ mm. To conduct the experiments, an electronic control electrical oven and vacuum saturation equipment were utilized. Three samples

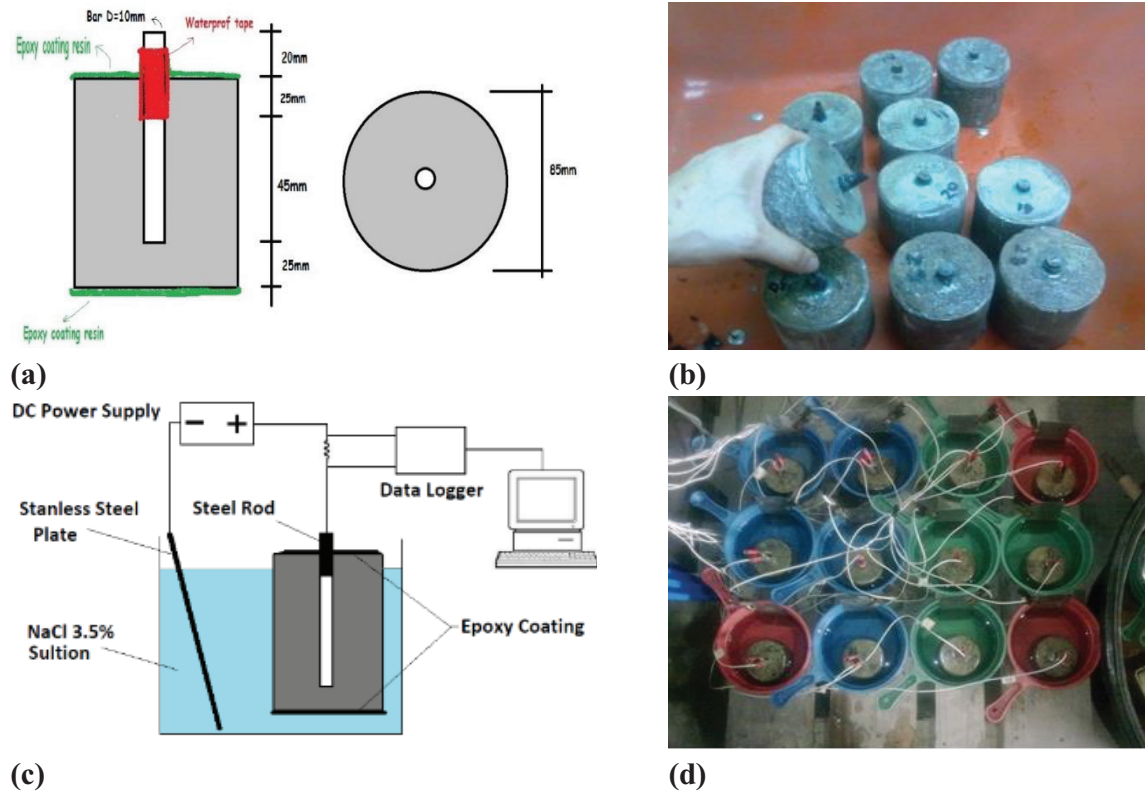
Bar D=10mm
Waterprof tape
Epoxy coating resin
20mm
25mm
45mm
25mm
85mm
Epoxy coating resin
(a)
(b)
DC Power Supply
− +
Data Logger
Stanless Steel Plate
Steel Rod
NaCl 3.5% Sultion
Epoxy Coating
(c)
(d)

Fig. 4. IVT procedure: (a) Sample preparation; (b) samples for the IVT; (c) the IVT schematic setup; (d) samples under the IVT

were examined for each group of tests at 7, 28, 60, and 90 days. The results reported were the average of three specimens. The values for water absorption and porosity were determined using Equations (1) and (2), respectively.

$$\text{Water absorption} = \frac{W_1 - W_2}{W_1} * 100 \qquad (1)$$

$$\text{Porosity} = \frac{W_1 - W_2}{W_1 - W_3} * 100 \qquad (2)$$

where: "W_1", "W_2", and "W_3" refer to the mass of the specimen, which was determined in a saturated surface-dry state while exposed to ambient air, under oven-dry conditions at about 105±5°C for a duration of 24 hours, and in water, respectively.

2.4.4. Impressed voltage test

The evaluation of the concrete durability in terms of chloride resistance was performed after 7, 28, 60, and 90 days of curing via the impressed voltage test (IVT). This test was applied by Topçu and Boğa [35] and Bignozzi and Bonduà [36] to examine the corrosion-resistant performance of reinforced concrete samples. The cylindrical samples used had a diameter of 85 mm and a height of 95 mm (Fig. 4a). All samples had a steel bar with a 10-mm diameter and a length of 115 mm embedded in the center, as shown in Fig. 4b. The tops and bottoms of the samples were coated with a non-active epoxy resin to prevent the penetration of chloride ions. A 15-volt direct current (DC) was used while immersing the samples in a 3.5% NaCl solution at the ages of 7, 28, 60, and 90 days, as carried out by Bignozzi and Bonduà [36]. Figure 4c shows the schematic diagram of the IVT setup to assess the resistance of the samples against corrosion, in which the bar served as the anode (working electrode) and a stainless-steel plate functioned as the cathode (counter electrode). A KYOWA UCAM-65B data logger was used to monitor the corrosion currents of the samples. The IVT setup of the samples is shown in Figure 4d. The samples

were observed regularly for the occurrence and progression of longitudinal cracks. The electrical resistance of the specimens was determined using the electrochemical Equation (3) provided below:

$$R = \frac{V}{I} \tag{3}$$

where:
R is resistance in ohms (Ω), V is potential in volts (v), and I is current in amperes (A).

2.4.5. Mass loss

The mass loss method is commonly used to estimate the corrosion resistance of reinforced concrete via the measurement of the corrosion rate. In this study, the mass loss of the samples was obtained after performing the IVT. The samples were visually examined for any existing cracks and then subjected to pressure using a compression machine. The function of the exerted pressure was to help break the specimens and facilitate the removal of the steel bars for the determination of the mass loss. The corroded steel bars were cleaned and weighed using a digital balance scale. The results reported were the average of three specimens. The corrosion rate (CR) measured in mm/year was determined using Equation (4):

$$CR = \frac{87.6 * W}{D * T * A} \tag{4}$$

where: "W" refers to the weight loss (mg) obtained by deducting the weights of the steel before and after the test; "D" refers to the density of the steel bar, which is equal to 7.86 g/cm^3; "T" refers to the time period of the corrosion test, measured in hours; and "A" is equal to 14.13 cm^2 and represents the corrosion area, which refers to the portion of rebar that is embedded within the sample and lacks a protective coating, therefore making it susceptible to corrosion.

3. Results and discussion

3.1. Physical and chemical properties of U-POFA

Table 2 displays the changes observed in the physical characteristics of the POFAs during all

Table 2. The physical characteristics of POFAs and OPC

Materials	OPC	O-POFA	G-POFA	U-POFA
Median particle size (μm)	10.18	16.66	12.35	2.21

stages. The U-POFA exhibited the smallest median particle size of 2.21 μm. When compared with the median particle sizes of the O-POFA and OPC, it is obvious that the U-POFA achieved a size reduction of 86.73% and 78.29%, respectively. Moreover, the SEM micrographs, which show the morphology of the particle size of the different types of POFA, are depicted in Figure 5 in which a notable reduction in the grain dimensions of the POFA particles can be seen at various phases of the treatment procedure. This aligns with the numerical outcomes presented in Table 2. The chemical compositions of OPC, G-POFA, and U-POFA determined via XRF analysis are presented in Table 3. The findings indicate that the treatment procedure resulted in an improvement in the chemical composition of the G-POFA and significantly reduced the carbon content by 85.4% (from 30.60% to 4.74%). In addition, a reduction of 87.12% was noticed in the content of the LOI between the G-POFA and the U-POFA. Thus, the treatment of POFA contributed to the enhancement of its chemical compositions and gave it significant potential to have superior resistance against corrosion and aggressive environmental conditions.

3.2. Slump test results

The slump results for all HSGC mixes are depicted in Figure 6. The data presented in the table indicate that when compared to the control concrete (i.e., OPC), the slump test value increases by 25 mm, 40 mm, and 45 mm for HSGC mixes 20UP, 40UP, and 60UP, respectively. The slump increased by 13.5%, 18.9%, and 21.6% for 20UP, 40UP, and 60UP, respectively, compared with OPC. However, the rate of increase has experienced a minor decrease compared to a lower rate of replacement percentage of U-POFA, which is similar to the finding reported in previous research [14].
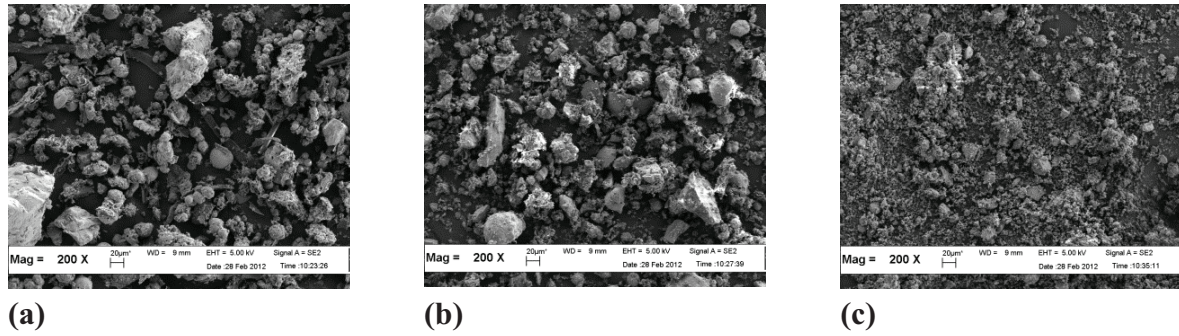
Fig. 5. SEM morphology of POFAs: (a) O-POFA; (b) G-POFA; (c) U-POFA

Table 3. The chemical compositions of OPC, G-POFA, and U-POFA

Compositions	OPC	G-POFA	U-POFA
SiO_2	18.81	45.37	62.08
Al_2O_3	4.54	5.09	7.09
Fe_2O_3	3.2	3.76	5.92
CaO	65.77	3.87	5.39
MgO	0.78	3.22	4.24
P_2O_5	0.08	2.99	3.84
K_2O	1.18	4.11	5.57
SO_3	3.54	0.23	0.23
TiO_2	0.20	0.19	0.27
MnO	0.19	0.06	0.09
Na_2O	0.09	0.07	0.10
C		30.60	4.74

Fig. 6. Slump results for all mixes

According to Johari et al. [14], the occurrence can be attributed to the U-POFA having a higher surface area and lower specific gravity in contrast to OPC. The inclusion of U-POFA in HSC leads to a larger paste volume of binder compared to HSC consisting only of OPC. As a result, the reduced grain size of U-POFA, as compared to OPC, may produce enhanced workability and slump rates. Hence, it is advisable to employ an elevated amount of U-POFA in order to reduce the dose of super-plasticizer or the water/binder ratio, contingent upon the target slump value.

3.3. Compressive strength results

As Figure 7 shows, the CS of HSGC speci-mens deteriorated significantly with the inclusion of the U-POFA, especially at an early 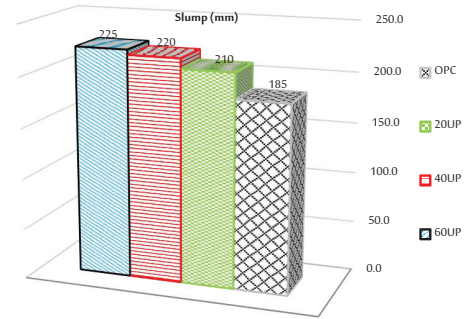age. For instance, at 7 days, the CSs of the 20UP, 40UP, and 60UP were 76.03 MPa, 70.63 MPa, and 60.1 MPa, respectively. Similar results were reported in a few related research reports [25]. The reason behind this deterioration might be due to the dilution effect caused by the partial replacement of OPC with U-POFA. However, with prolonged curing, the percentage of relative strength of the U-POFA specimens increased and surpassed that of the OPC sample as a result of the pozzolanic reaction between the U-POFA and calcium hydroxide (CH). After a period of 90 days, the findings indicate that the strength of the HSGC exhibits improvements when U-POFA is used as a replacement for OPC by 20%, 40%, and 60%. This suggests that incorporat-ing U-POFA in high volume has a positive impact on the CS of HSGC. Meanwhile, it is evident that a substitution of up to 60% U-POFA in terms of weight of OPC has the potential to improve the CS of the HSGC to a comparable extent as concrete consisting only of 100% OPC after a period of 90 days, as shown in Figure 7a. With U-POFA
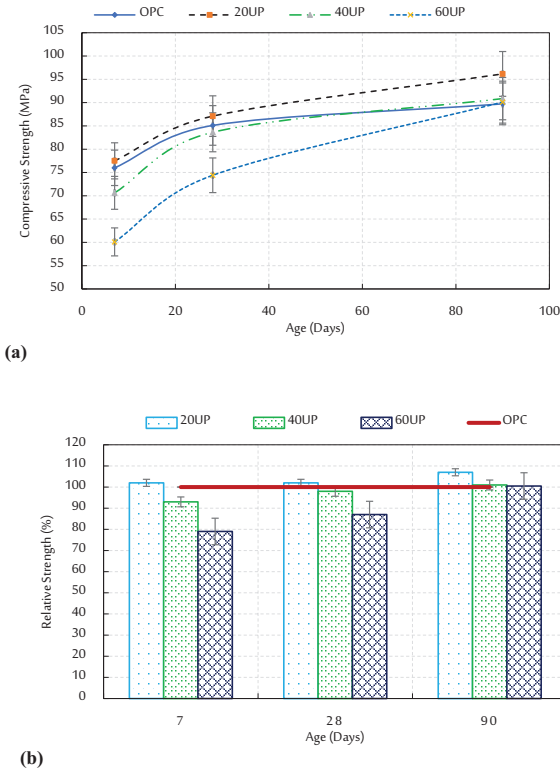
(a)

(b)

Fig. 7. Compressive strength results: (a) strength development with days; (b) the relative strength

replacing 20% of OPC, Figure 10b shows that the CS of the concrete specimens is higher after 7 and 28 days, though only slightly higher than the concrete made with 100% OPC. Nevertheless, after 90 days, the strength exhibits a notable increase. Despite observing a decrease in CS at 7 and 28 days when the replacement rate of OPC was increased to 40%, a slightly higher CS was recorded at 90 days compared to the control concrete. The HSGC's strength decreased more when 60% of U-POFA was added, and this decrease is more noticeable at 7 and 28 days of curing compared to all other samples. It is noteworthy, however, that the strength continues to increase from 7 to 28 days. Nevertheless, after a curing period of 90 days, the 60UP mixture exhibited a CS that was comparable to that of the OPC concrete and approached nearly the same level of CS, as shown in Figure 7. However, it is important to mention that according to this study, the utilization of 20% substitution of U-POFA did not result in a reduction of CS over the 7, 28, or 90

days. In fact, it significantly improved the strength. Hence, in situations where there is a requirement for enhanced CS during the early ages, it is advisable to ascertain and implement the optimal volume of U-POFA replacement. In this investigation, it has been shown that a replacement dose of 20% is indicated. Similar results were reported by several researchers in related studies [17]. Jaturapitakkul et al. [15] observed the effect of fineness and filler effects on the enhancement of CS in concrete, including concrete incorporating G-POFA. Therefore, in order to achieve this objective, it is crucial to examine at least two key aspects. Firstly, the utilization of SCM possessing enhanced pozzolanic characteristics has the potential to increase the formation of calcium silicate hydrate (C-S-H) in the cement pastes. This phenomenon holds significant advantages in terms of enhancing concrete strength. This particular possibility arises within the context of HSGC that incorporates SCMs. Additionally, the second component to consider is the particle size of the pozzolanic materials, whereby smaller particles contribute to the formation of a denser microstructure via the micro-filler effect [25]. Based on previous studies, increasing the replacement content to 60% by weight of OPC led to a minor decrease in the CS , which was 105.2.5, 109.9, and 108.6 MPa, to replacement rates of 20%, 40%, and 60%, respectively [14]. This is consistent with the results obtained in this study, which indicate that a replacement rate of 60% by weight may be sufficient to maintain high CS in addition to satisfactory transport and durability properties. CS, in addition to durability, is an important characteristic and criterion for producing HSGC [25].

3.4. Water absorption and porosity

Table 4 presents the water absorption and porosity results of all HSGC mixes. Based on the porosity test findings presented in Table 4, the OPC concrete sample exhibited a porosity of 12.3% after 7 days of curing. In contrast, the 20UP, 40UP, and 60UP samples displayed porosities of 11.6%, 9.6%, and 8.8%, respectively, with reduction percentages compared to the OPC sample of 5%, 22%,

Table 4. Porosity and water absorption results

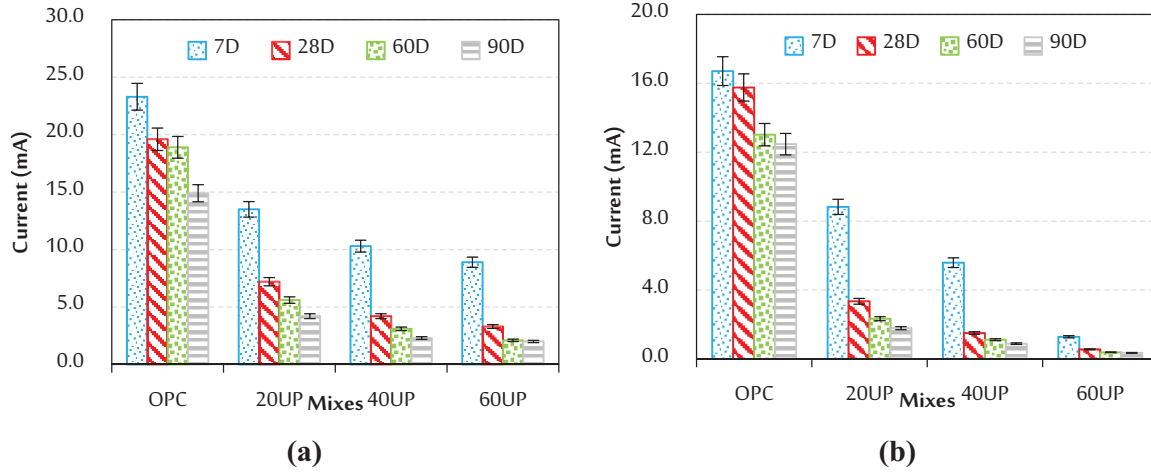| Mix	OPC			20UP			40UP			60UP		
Age (days)	7	28	90	7	28	90	7	28	90	7	28	90
Porosity (%)	12.3	10.9	10.1	11.6	9.5	8.7	9.6	9.2	7.4	8.8	7.4	5.4
Water absorption (%)	5.7	4.8	4.2	5.0	4.1	3.7	4.3	4.0	3.2	3.8	3.2	2.3

Fig. 8. Impressed voltage test results: (a) the initial current of samples; (b) the average steady state currents

and 28%, respectively. Looking at the results after 28 days of curing, it is evident that the samples of all HSGC mixes that contain U-POFA become less porous as the curing time increased. The reduction values reached 13%, 15%, and 32% for 20UP, 40UP, and 60UP, respectively, as compared to the OPC specimens. In the case of the porosity after 90 days, the reduction values reached 23%, 36%, and 47% for 20UP, 40UP, and 60UP, respectively, as compared to the OPC sample. The significant decrease in porosity clearly illustrates that the use of U-POFA has the capacity to effectively diminish the porosity of HSGC. Moreover, the findings of the present study align well with those of related prior research works [14]. These studies suggest that the fineness of POFA has a direct impact on pore size, indicating that increased fineness can effectively mitigate the aforementioned problems. Therefore, it can be observed that the HSGC incorporating U-POFA demonstrates a reduced porosity rate when subjected to a longer curing period as compared to OPC concrete. Achieving a larger decrease rate can be accomplished by employing higher replacement levels of U-POFA. Regarding

the water absorption after 7 days of curing, the reduction values reached 11%, 24%, and 33% for 20UP, 40UP, and 60UP, respectively, as compared to the OPC sample. The same trend was noticed after 28 days of curing, where the reduction values reached 15%, 16%, and 34% for 20UP, 40UP, and 60UP, respectively, as compared to the OPC sample. Moreover, after 90 days of curing, the 20UP, 40UP, and 60UP exhibited reduction values of 22%, 34%, and 45%, respectively, as compared to the OPC sample, as shown in Table 4. Therefore, it can be shown that the water absorption of HSGC samples follows a similar trend to the porosity. Specifically, as the samples age and the U-POFA replacement level increases, the water absorption decreases in contrast to the samples containing OPC. Similar results were reported by several researchers, such as Kroehong et al. [37].

3.5. Impressed voltage test

Figure 8a depicts the average initial currents of the samples obtained from the IVT. It is evident that the initial currents of the OPC samples were

Table 5. Impressed voltage test results (in hours)

Mix	The start–end times of steady state				The initial crack time of the samples			
Age (Days)	7	28	60	90	7	28	60	90
OPC	40 – 180	40 – 190	35 – 230	20 – 240	176	188	229	236
20UP	40 – 230	30 – 350	10 – 477	5 – 477	234	353	–	–
40UP	35 – 245	20 – 477	5 – 477	1 – 477	245	–	–	–
60UP	25 – 477	15 – 477	1 – 477	0.5 – 477	–	–	–	–

the highest at all ages. For instance, at 7 days, the initial current of the OPC specimen was the highest at 23.3 mA, over the experiment, the 20UP, 40UP, and 60UP had initial currents of 13.5 mA, 10.3 mA, and 8.9 mA, respectively. The same trend was also noticed at the other three ages. Therefore, it can be concluded that the initial current was inversely proportional to the amount of U-POFA in the mixtures, indicating that the use of U-POFA enhanced the permeability properties of the HSGC., that is, making the concrete more impermeable. Similar results were reported by Topçu and Boğa [35], who reported that including 10% and 20% fly ash as a replacement for OPC decreases the primary currents and corrosion rate in comparison to concrete zero-FA. The reduction in the initial current of HSGCs with the inclusion of U-POFA could be linked to the refinement in the pore structure of the HSGC containing U-POFA as a result of its effective pozzolanic reaction with CH to produce C-S-H, particularly at higher contents of U-POFA. Earlier, Johari et al. [14] reported significant improvement of transport properties of HSGC containing U-POFA. Hence, the results of the current study corroborate the findings of Johari et al. [14] on the improvement of the HSGC transport properties after the inclusion of U-POFA. The steady state of the current time was also measured on the basis of the start and end times of the IVT. Okba et al. [38] stated that the longer the steady state of the current time during testing, the better the corrosion resistance of the concrete is. Table 5 and Figure 8b present the start-end times of the steady state and the average currents at the steady state, respectively. The results show that the OPC sample exhibited the shortest durations with the highest currents at both initial and steady state stages compared with the samples

containing U-POFA at all ages. This proves that the corrosion-resistant performance of the HSGCs containing U-POFA is superior to that of the OPC specimen, with much superior corrosion-resistant performance at higher contents of U-POFA. Okba et al. [38] noticed a sharp rise in the current during the IVT measurements, accompanied by multiple simultaneous cracks in the samples. In this study, the sharp rising phases with crack time were investigated. Figure 9 shows the cracks that occurred during the IVT at 7, 28, 60, and 90 days. The occurrence time of the initial cracks is indicated by arrows (Fig. 10) and illustrated in Table 5. Figure 9 and Table 5 show that all the OPC samples at 7, 28, 60, and 90 days. Conc20133 experienced cracks after 176 h, 188 h, 229 h, and 236 h, respectively. It is noticed that the time to the initial crack increased with age (curing time) due to the reduction in porosity and the increase in strength of the samples with continued hydration over a longer curing period. This improvement can be clearly noticed in the specimens with U-POFA, which could be attributed to the refinement in the structure of the pores as a result of the pozzolanic reaction of the U-POFA, especially when the replacement level of U-POFA is high. At 7 and 28 days, the 20UP samples cracked after 234 h and 353 h, respectively, but no sign of cracks was detected at 60 and 90 days. Chindaprasirt et al. [39] employed the G-POFA to enhance the corrosion resistance of HSC with replacement levels of 10, 20, and 30% by mass of OPC at 7, 28, and 90 days. At a 20% replacement level, the cracks were initiated after 180 h, 220 h, and 275 h at 7, 28, and 90 days, respectively. By comparing the results, the inclusion of U-POFA in this study delayed the crack time by 23%, 38%, and 100% at 7, 28, and 90 days, respectively.
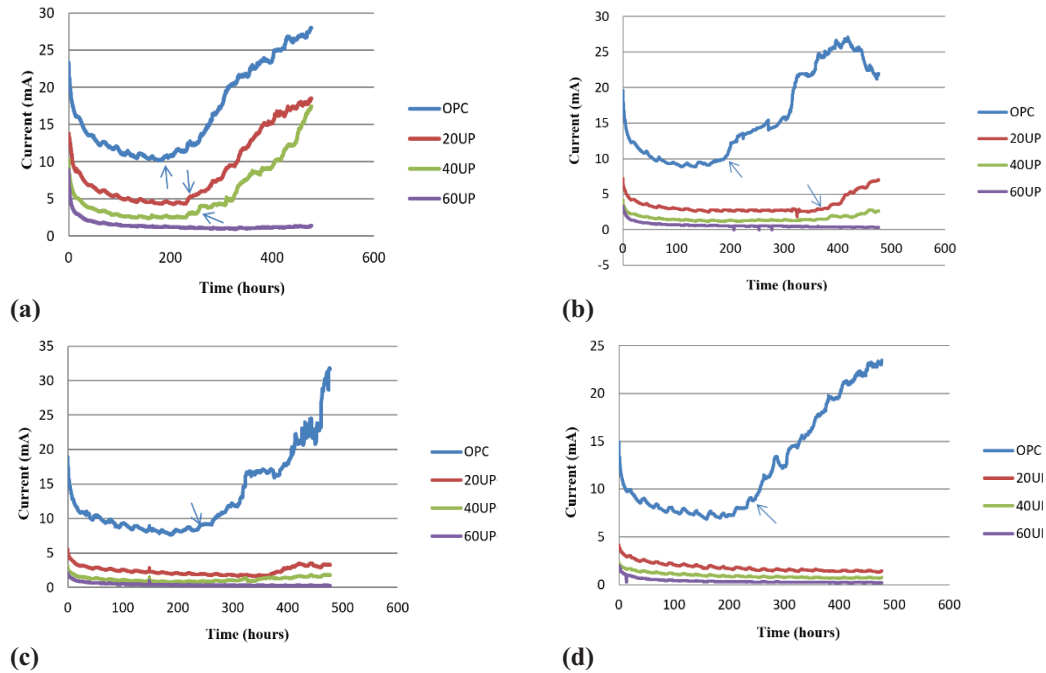
Fig. 9. The corrosion current vs time of the specimens at: (a) 7 days; (b) 28 days; (c) 60 days; (d) 90 days

This indicates that U-POFA is more efficient than the G-POFA in terms of enhancing the corrosion resistance of HSC. For the 40UP samples, a crack only occurred after 245 h, i.e., at 7 days. In the case of the 60UP samples, however, no crack was observed at any age, serving as more evidence that increasing the volume of the U-POFA contributed greatly to the prevention of corrosion and the formation of cracks.

3.6. Mass loss

Table 6 presents the rates of corrosion determined for the OPC, 20UP, 40UP, and 60UP specimens at 7, 28, 60, and 90 days. The results show that the rates of corrosion decreased with the increase in U-POFA content at all ages of the HSGCs. Compared with the corrosion rate of the OPC at 7 days, those of the 20UP, 40UP, and 60UP decreased by 46%, 67%, and 91%, respectively. The corrosion rates observed for OPC, 20UP, 40UP, and 60UP specimens at the 28-day mark were 6.945, 1.488, 0.717, and 0.331 mm/year, respectively. The observed reductions in corrosion rate for the 20UP, 40UP, and 60UP samples were approximately 79%, 90%, and 95% of the corrosion rate exhibited by the OPC sample. The same behavior was displayed at 28, 60, and 90 days. This could be attributed to the fact that the U-POFA decreased the pore size and permeability of the concrete via the pozzolanic reaction, resulting in lower currents and corrosion rates. Figure 10 depicts all the samples after the mass loss test. The presence of corrosion products is evident for the OPC sample, and the reinforcement bar exhibits a significant degree of corrosion, as shown in Figure 10a. Based on the visual analysis of the 20UP sample, it is readily apparent that the reinforcement exhibits a relatively confined degree of corrosion, as shown in Figure 10b. It can be noticed that the amount of corrosion on the reinforcement bars of the 40UP and 60UP specimens is almost negligible to none, as shown in Figure 10c, d.

3.7. SEM analysis

SEM micrographs in Figure 10 illustrate the effect of incorporating U-POFA as a substitute for OPC, with varying proportions of 0%, 20%, 40%, and 60% by weight, on the microstructural characteristics. From the morphology shown
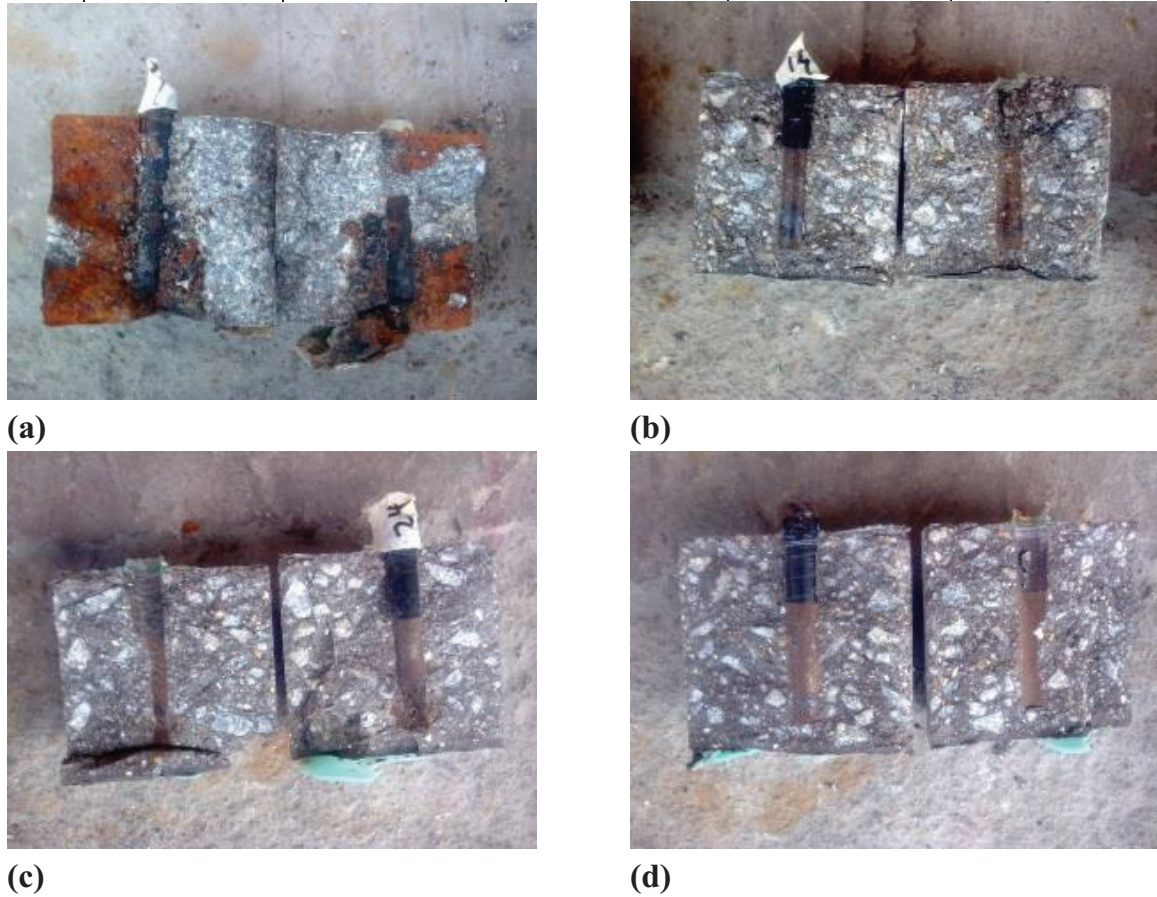
Fig. 10. Samples after the IVT: (a) OPC; (b) 20UP; (c) 40UP; (d) 60UP

Table 6. Corrosion rate (mm/ year) by mass loss via the IVT

Age (Days)	Mix			
	OPC	20UP	40UP	60UP
7	7.276	3.913	2.425	0.661
28	6.945	1.488	0.717	0.331
60	5.705	1.075	0.524	0.220
90	5.457	0.827	0.441	0.165

in Figure 11a–d, it is observed that the microstructures of cement paste have different shapes, and the changes in the microstructures depend on the rate of replacement of U-POFA with OPC. It is evident that the rise in the rate of OPC replacement by U-POFA led to an improvement in the microstructure with higher density (low permeability) through a decrease in the pore size and bonding of the cement paste compared to the cement paste zero-U-POFA or low content (20%) U-POFA. Two main compounds are made when OPC hydrates: C-S-H gel and CH. Utilizing supplementary cementitious materials like U-POFA typically has a substantial influence on the microstructures of the cement paste matrix [14]. The utilization of the ultrafine pozzolanic material enhances and purifies minute structures at a microscopic level. The large amount of silicon dioxide (SiO_2) and noncrystalline aluminum oxide (Al_2O_3) in the POFA causes a chemical reaction with CH, leading to the creation of calcium silicate hydrate (C-S-H), calcium alumino-silicate hydrate (C_2ASH_8), and calcium aluminate hydrate (C_4AH_{13}). The pozzolanic reaction has a dual effect: it reduces the quantity of CH, while increasing the quantities of C-S-H and C_2ASH_8, and thus lowering the amount of ettringite [16, 24]. The interaction between CH and amorphous SiO_2 and Al_2O_3 leads to the creation of supplementary
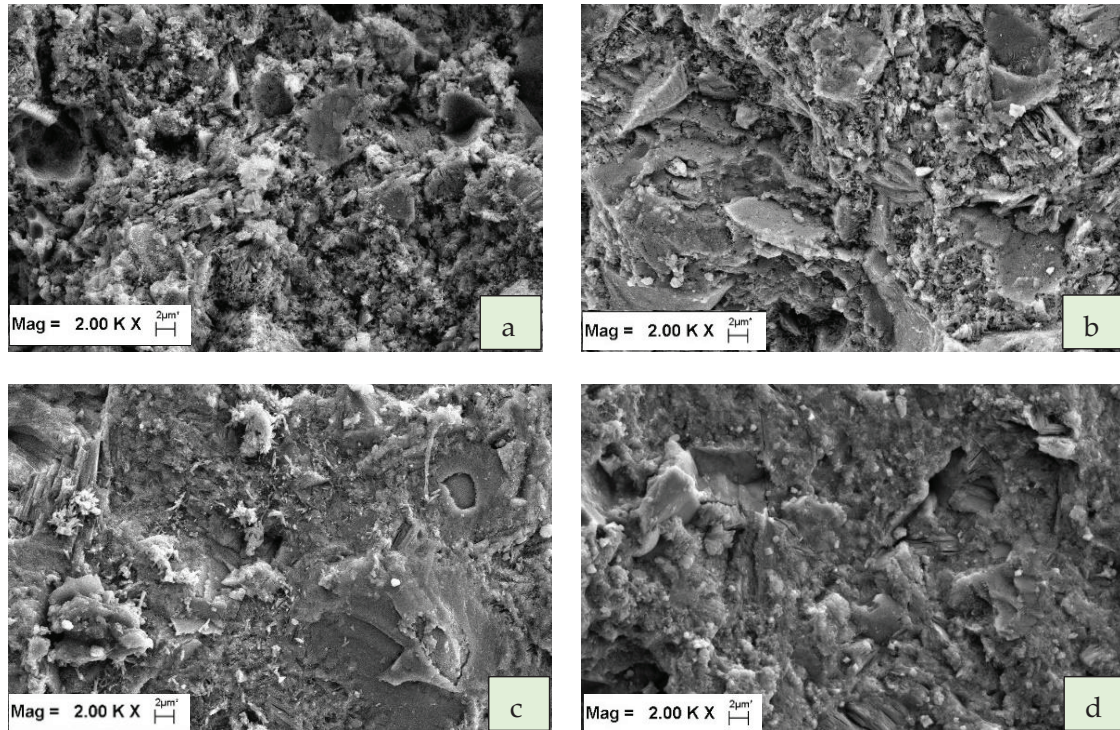
Fig. 11. SEM imaging of cement pastes aged 28 days, (a)Cement paste contains 0% U-POFA, (b) Cement paste contains 20% U-POFA, (c) Cement paste contains 40% U-POFA, (d) Cement paste contains 60% U-POFA

C-S-H and calcium-aluminate-silicate-hydrate (C-S-A-H) gels. This technique further improves the microstructure and plugs the pores.

4. Conclusions and recommendations

According to the research findings, it is possible to offer the following conclusions:

1. The U-POFA exhibited the smallest median particle size of 2.21 μm and achieved a size reduction of 78.29% in comparison with that of the OPC.

2. The XRF analysis displayed that the treatment process enhanced the chemical composition of the G-POFA and significantly reduced the carbon content by 85.4%.

3. Adding U-POFA enhances the workability of mixes, where an increased quantity of U-POFA can further augment the slump and, thus, the workability.

4. The substitution of OPC with 40% and 60% by weight of U-POFA exhibited a reduction in the CS of the HSGC specimens at an early age. However, using those levels showed better or similar long-term CS.

5. Using 20% U-POFA can make the CS much higher at a young age than HSC made with 100% OPC.

6. The porosity and water absorption results show that specimens incorporating U-POFA demonstrate jreduced porosity and water absorption rate when subjected to a longer curing period as compared to OPC concrete. Achieving a larger decrease rate can be accomplished by employing higher replacement levels of U-POFA.

7. The IVT showed that the initial current was inversely proportional to the amount of U-POFA, indicating that the U-POFA improved the permeability characteristics of the concrete.

8. The OPC sample exhibited the shortest durations with the highest currents at both initial and steady-state stages compared with the samples containing U-POFA at all ages. In other words, the greater the U-POFA content, the better the corrosion resistant performance will be.

9. It is noticed that the time to the initial crack increased with the curing time due to the reduction in porosity and increase in strength from the prolonged curing time.

10. The results show that the corrosion rates of the HSGCs decreased with the increase in U-POFA content at all ages. This could be linked to the fact that the U-POFA decreased the pore size and permeability of the concrete via the pozzolanic reaction, resulting in lower currents and corrosion rates.

In general, it is strongly advised to incorporate U-POFA with 60% of the OPC content. This is due to its significance as an environmentally friendly and cost-effective green pozzolanic material, which significantly improves the corrosion resistance properties of HSGC. Hence, it could contribute to the superior durability performance of concrete structures, particularly in aggressive environmental exposures.

The high durability and resistance to aggressive environments of concrete are important aspects that allow concrete to be widely used in harsh infrastructure conditions to ensure a longer lifespan. As a result, more research into these aspects is required in the future:

1. Monitoring the corrosion current of concrete containing U-POFA through the use of accurate on-site evaluation devices.

2. Conducting a comprehensive study by analyzing the various parameters of the micro-IVT test and the PGStat device in both potential and galvanic methods, in addition to impedance spectroscopy.

3. Monitoring the corrosion current of concrete exposed to a harsher environment (high acid and sulfate concentrations).

4. Further research investigated the microstructural characteristics of HCG cement pastes containing UPOFA.

Acknowledgments

Conflicts of Interest

The authors declare no conflict of interest.

References

[1] Holland RB, Kurtis KE, Kahn LE. Effect of different concrete materials on the corrosion of the embedded reinforcing steel. In: Poursaee A, editor. Corrosion of steel in concrete structures. Cambridge, MA: Woodhead Publishing [Elsevier imprint]; 2023: p. 199–218.

[2] Zhao, Y., Pan T, Yu X, Chen D. Corrosion inhibition efficiency of triethanolammonium dodecylbenzene sulfonate on Q235 carbon steel in simulated concrete pore solution. *Corros Sci*. 2019;158:108097.

[3] Zeyad AM. Effect of harsh environment on cement mortar containing natural pozzolans. *Case Stud Constr Mater*. 2024;20:e02808.

[4] Liang Y, Wang L. Prediction of corrosion-induced cracking of concrete cover: a critical review for thick-walled cylinder models. *Ocean Eng*. 2020;213:107688.

[5] Jagadesh P, Ramachandramurthy A, Rajasulochana P, Hasan MA, Murgesan R, et al. Effect of processed sugarcane bagasse ash on compressive strength of blended mortar and assessments using statistical modelling. *Case Stud Constr Mater*. 2023;19:e02435.

[6] Garg R, Garg R, Eddy NO, Khan MA, Khyan AH, Alomavri T, Berwal P. Mechanical strength and durability analysis of mortars prepared with fly ash and nano-metakaolin. *Case Stud Constr Mater*. 2023;18:e01796.

[7] Paruthi S, Khan AH, Kumar A, Kumar F, Hasan MA, Magbool HM, Manzar MS. Sustainable cement replacement using waste eggshells: a review on mechanical properties of eggshell concrete and strength prediction using artificial neural network. *Case Stud Constr Mater*. 2023;18:e02160.

[8] Al-Akhras NM. Durability of metakaolin concrete to sulfate attack. *Cem Concr Res*. 2006;36(9):1727–34.

[9] Zeyad AM, Johari MAM, Abadel A, Abutaleb A, Mijarsh MJA, Almalki A. Transport properties of palm oil fuel ash-based high-performance green concrete subjected to steam curing regimes. *Case Stud Constr Mater*. 2022;16:e01077.

[10] Ranjbar N, Mehrali M, Alengaram UJ. Compressive strength and microstructural analysis of fly ash/palm oil fuel ash based geopolymer mortar. *Mater Des*. 2014;59:532–9.

[11] Mujah D. Compressive strength and chloride resistance of grout containing ground palm oil fuel ash. *J Clean Product*. 2016;112:712–22.

[12] Chindaprasirt P, Homwuttiwong S, Jaturapitakkul C. Strength and water permeability of concrete containing palm oil fuel ash and rice husk–bark ash. *Constr Build Mater*. 2007;21(7):1492–9.

[13] Hamada H, Alattar A, Tayeh B, Yahaya F. Sustainable application of coal bottom ash as fine aggregates in concrete: a comprehensive review. *Case Stud Constr Mater*. 2022;16:e01109.

[14] Johari MAM, Zeyad AM, Muhamad Bunnori N, Ariffin KS. Engineering and transport properties of high-strength green concrete containing high volume of ultrafine palm oil fuel ash. *Constr Build Mater*. 2012;30:281–8.

[15] Jaturapitakkul C, KIattikomol KI, Tangchirapat W. Evaluation of the sulfate resistance of concrete containing palm oil fuel ash. Constr Build Mater. 2007;21(7):1399–405.

[16] Chandara C, Aziozio KAM, Ahmad ZA, Hashim SFS, Sakai E. Heat of hydration of blended cement containing treated ground palm oil fuel ash. *Constr Build Mater*. 2012;27(1):78–81.

[17] Zeyad, AM, Megat Johari MA, Tayeh BA, Olalekan Yusuf M. Efficiency of treated and untreated palm oil fuel ash as a supplementary binder on engineering and fluid transport properties of high-strength concrete. Constr Build Mater. 2016;125:1066–1079.

[18] Thomas N, Mathew S, Nair KM, O'Dowd K, Forouzandeh P, Goswami A, et al. 2D MoS2: structure, mechanisms, and photocatalytic applications. *Mater Today Sustain* 2021;13:100073.

[19] Hamada HM, Jokhio GA, Yahaya F, Humada AM, Gul Y. The present state of the use of palm oil fuel ash (POFA) in concrete. *Constr Build Mater*. 2018;175:26–40.

[20] Hamada HM, Al-Attar A, Shi J, Yahaya F, Al Jawahery MS, Yousif ST. Optimization of sustainable concrete characteristics incorporating palm oil clinker and nano-palm oil fuel ash using response surface methodology. *Powder Technol*. 2023;413:118054.

[21] Alsubari B, Shafigh P, Ibrahim Z, Alnahhal F, Jumaat MZ. Properties of eco-friendly self-compacting concrete containing modified treated palm oil fuel ash. *Construct Build Mater*. 2018;158:742–54.

[22] Alani AH, Bunnori NM, Noaman AT. *D*urability performance of a novel ultra-high-performance PET green concrete (UHPPGC). *Constr Build Mater*. 2019;209:395–405.

[23] Alsubari B, Shafigh P, Jumaat MZ. *D*evelopment of self-consolidating high strength concrete incorporating treated palm oil fuel ash. *Materials*. 2015;8(5):2154–73.

[24] Bassuoni MT, Nehdi ML. Resistance of self-consolidating concrete to sulfuric acid attack with consecutive pH reduction. *Cem Concr Res*. 2007;37(7):1070–84.

[25] Zeyad AM. Pozzolanic reactivity of ultrafine palm oil fuel ash waste on strength and durability performances of high strength concrete. *J Clean Prod*. 2017;144:511–22.

[26] Hassan MH, Abo Sabah SH, Bunnori NM, Megat Johari, MA. Fluid transport properties of normal concrete substrate and a new green fiber reinforced concrete overlay composite. *Struct Concr*. 2019;20(5):1771–80.

[27] ASTM-C150. Standard test method for Portland cement. 2016, West Conshohocken, PA, United States.

[28] ASTM-C128. Standard test method for relative density (specific gravity) and absorption of fine aggregate. 2015, West Conshohocken, PA, United States.

[29] ASTM-C136. Standard test method for sieve analysis of fine and coarse aggregates. 2006, West Conshohocken, PA, United States.

[30] ASTM-C127. Standard test method for relative density (specific gravity) and absorption of coarse aggregate. 2015, West Conshohocken, PA, United States.

[31] ASTM-C33/C33M. Standard specification for concrete aggregates. 2018.

[32] ASTM-C496. Standard test method for splitting tensile strength of cylindrical concrete specimens. West Conshohocken, Pennsylvania, USA. 2011.

[33] EN B. 12390-3, Testing hardened concrete-Part 3: Compressive strength of test specimens. British Standards Institution, 2002.

[34] ASTM-C373, Standard test method for water absorption, bulk density, apparent porosity, and apparent specific gravity of fired whiteware products. ASTM International, West Conshohocken, Pennsylvania, USA. 2014.

[35] Topçu İB, Boğa AR. Effect of ground granulate blast-furnace slag on corrosion performance of steel embedded in concrete. *Mater Des*. 2010;31(7):3358–65.

[36] Bignozzi MC, Bonduà S. Alternative blended cement with ceramic residues: corrosion resistance investigation on reinforced mortar. *Cem Concr Res*. 2011;41(9):947–54.

[37] Kroehong W, Sinsiri T, Jaturapitakkul C. Effect of palm oil fuel ash fineness on packing effect and pozzolanic reaction of blended cement paste. *Proc Eng*. 2011;14:361–9.

[38] Okba SH., A.S. El-Dieb, and M.M. Reda MM. Evaluation of the corrosion resistance of latex modified concrete (LMC). *Cem Concr Res*. 1997;27(6):861–8.

[39] Chindaprasirt P, Chotetanorm C, Rukzon S. Use of palm oil fuel ash to improve chloride and corrosion resistance of high-strength and high-workability concrete. *J Mater Civil Eng*. 2011;23(4):499–503.